ELSEVIER

Colloids and Surfaces
A: Physicochemical and Engineering Aspects 208 (2002) 187–198

COLLOIDS AND SURFACES A

www.elsevier.com/locate/colsurfa

Collision induced processes at the gas–surface interface

Micha Asscher [a,*], Leonid Romm [b], Yehuda Zeiri [c]

[a] *Department of Physical Chemistry and The Farkas Center for Light Induced Processes, The Hebrew University, Jerusalem 91904, Israel*
[b] *Department of Chemistry, University of California, Berkeley, CA 94720, USA*
[c] *Department of Chemistry, Nuclear Research Center Negev, P.O. Box 9001, Beer-Sheva 84190, Israel*

Received 27 June 2001; accepted 5 December 2001

Abstract

The collision of energetic gas phase particles with adsorbed species can induce a variety of processes. Events of this kind can play an important role in the mechanisms governing heterogeneous catalysis at high pressures and elevated temperatures. Two collision induced processes (CIP) are described in this article. The first process discussed is collision induced desorption (CID). The CID of N_2 from Ru(001) is considered at both low and high coverage ranges. The interpretation of the experimental data using molecular dynamics (MD) simulations leads to the introduction of a new desorption mechanism involving surface corrugation and adsorbate frustrated rotational motion. The second process is collision induced migration (CIM), an event that has never been considered before neither experimentally nor theoretically. It is demonstrated, using MD simulations, that following energetic CIM, very long distances of more than 100Å can be covered by the adsorbates at low coverages. At high coverages, on the otherhand, these displacements become considerably shorter due to surface collisions with neighbors. © 2002 Elsevier Science B.V. All rights reserved.

Keywords: Gas–surface dynamics; Collision induced desorption; Collision induced migration

1. Introduction

The collision of energetic gas phase particles with adsorbates on solid surfaces can induce several different processes. The attempt to understand the detailed mechanism of collision induced phenomena has been a focus of interest for more than a decade. Early molecular dynamics (MD) simulations demonstrated that detailed study of collision induced desorption (CID) may be used as a direct probe of adsorbate–substrate interaction potential [1]. Following this numerical simulation, numerous experiments have shown that energy transfer from a projectile to the adsorbate–surface system can lead to desorption [2–13] and dissociation [12–17] of the adsorbed species. In addition, experiments have demonstrated the possibility for unimolecular [18] and bimolecular [19] reactions on solid surfaces induced by hyperthermal projectiles. More recently, it was also demonstrated that collision of rare gas atoms with the H–Ni(111) system results in the transition of

* Corresponding author.

0927-7757/02/$ - see front matter © 2002 Elsevier Science B.V. All rights reserved.
PII: S0927-7757(02)00145-0

the hydrogen from its adsorbed state to a subsurface site [20–22]. Moreover, both experiments [23–28] and simulation [29,30] demonstrated that 'hot' atoms generated in the photo-dissociation of an adsorbate can lead to CID or dissociation of a neighboring adsorbate. The initial conditions for the projectile–adsorbate scattering event in these systems are dictated by the arrangement of the adsorbates on the surface. Hence, this type of events was termed localized atomic scattering (LAS) [23,24,30]. A variety of numerical simulations, including simple hard cube models [5,6,8] as well as moderate [8,30–34] and large-scale [35,36] classical MD simulations, accompanied these experiments. The interest in collision induced surface processes is largely due to the possibility to relate ultra high vacuum (UHV) results to the outcome of measurements at high pressures. In particular, activated collision induced processes (CIP) , that have a reasonable rate only at high pressures, can be simulated in UHV using energetic projectiles to overcome the pressure gap [37].

The number of particles colliding with the surface increases linearly as a function of pressure. However, only a small fraction has high enough energy to induce most of the phenomena described above. The flux of gas particles colliding with an adsorption site on the surface is given by $F = P/(N_S(2\pi m k_B T)^{1/2})$, where P is the pressure, m mass of gas particles, T_g the gas temperature, k_B is Boltzman constant and N_S number of adsorption sites in a unit surface area. For most metal surfaces N_S is of the order of 10^{15} sites per cm^2, hence, at room temperature and $P = 760$ Torr the flux of argon atoms colliding with a given site on the surface will be $F = 2.44 \times 10^8\ s^{-1}$. Assuming that the kinetic energy of the gas atoms is governed by Boltzman distribution at $T_g = 300$ K, only one particle in the flux cited above has energy of 0.5 eV and only one out of 10 particles has energy of 1 eV. The number of energetic particles hitting a given site on the surface can be compared with the 'turnover number', TN (defined as the number of product molecules generated on a unit area of catalyst in a unit time).

For most heterogeneously catalyzed reactions under typical conditions of 400–800 K and upto 100 atmospheres of reactant pressure TN varies in the range 10^{-2}–$10^2\ s^{-1}$ [38]. This range of typical TN values is similar to the number of particles with energy upto about 0.75 eV that collide with an adsorption site during 1 s (using temperature and reactant pressure ranges described above). Hence, CIP may be an important route to obtain reaction products in heterogeneous catalysis, provided that the magnitude of the activation energy associated with the rate determining step is low enough and can be supplied by the projectile. The large value of F suggests that the probability that low activation energy processes will actually take place may be strongly pressure dependent. One such process is surface diffusion of adsorbates. The energy barrier for diffusion (E_{diff}) spans a wide range from zero upto about 1 eV, but for many industrially important systems E_{diff} is of the order of 0–0.3 eV. MD simulations show that for such low activation energies it is expected that the high collision rate of gas particles on the surface at atmospheric pressure will have a pronounced influence on the diffusion process [39].

The purpose of this article is to describe our approach to CIP. The emphasis in the discussion below will be on the detailed mechanism underlying these CIP. The details of the involved mechanisms will be based on both experimental findings and computer simulations of the different events. We shall start by describing the CID of N_2 from Ru(001) surface [9,32]. Unlike the case of spherically symmetric adsorbates, where the CID results can be explained using hard cube models, here, the desorption mechanism, involves a more complicated sequence of energy transfer events among different modes. The same system will be used to discuss a new type of CIP, namely, collision induced migration (CIM) [33]. In all these examples, we shall not discuss the details of the experimental or theoretical procedures. The emphasis will be on a description of the basic molecular-atomic level mechanism involved. For a comprehensive description of the experimental or theoretical details the reader is referred to the references cited above.

2. Collision induced desorption: the Ar–N_2–Ru(001) system

In the following we discuss the details of CID in the system Ar–N_2–Ru(001). The discussion will start by examination of the CID event at the low N_2 surface coverage limit. In this limit experimental data is available as well as computer simulations where a single adsorbate is considered. The second part of this section will discuss the CID process when surface coverage is increased. The high coverage regime is described theoretically by employing MD simulations.

2.1. Low coverage

The basic quantity measured experimentally and calculated in the simulations is the cross section, σ_{des}, for the CID process. It is obtained for a set of incidence energies (E_{in}), projectile angle of incidence (θ_{in}) and surface coverage value (Θ). The cross section for CID is defined as was previously suggested by Beckerle et al. [4] as an area on the surface within which an impact of rare gas atom yields a CID event per one adsorbed nitrogen molecule. The experimental cross section is derived from the exponentially decaying CID signal obtained when low coverage $^{15}N_2$ is exposed to a supersonic beam of Ar atoms (or Kr) seeded in He [9]. The experimental and theoretical results obtained for normal approach of the collider are presented in Fig. 1.

Due to experimental limitations, Ar was used as projectile for E_{in} upto 2.25 eV (open up triangles) while for larger E_{in} values Kr was used (open circles). This data should be compared with the corresponding calculated results with Ar and Kr as collider (filled up triangles and circles, respectively). Both experiment and simulation indicate that the CID process has a threshold energy, $E_{in} = E_{thr}$, below which no desorption is observed. For the N_2–Ru(001) system both experiment and simulation yield $E_{thr} = 0.5$ eV. This value of E_{thr} is about twice the magnitude of the adsorbate–surface binding energy. Moreover, that the magnitude of E_{thr} is independent of the incidence angle [9], see discussion below. Comparison between the

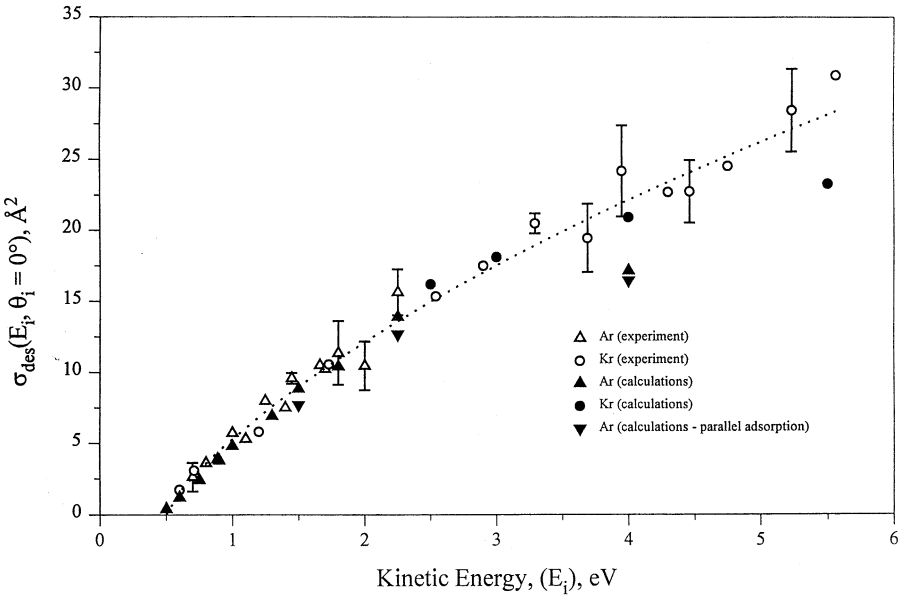

Fig. 1. σ_{des} As a function of incidence collider energy: experimental (open symbols), calculated for normal adsorption geometry (filled symbols), calculated for parallel adsorption geometry (filled symbols). The dotted line through the experimental data points is based on an expression described in [9–11].

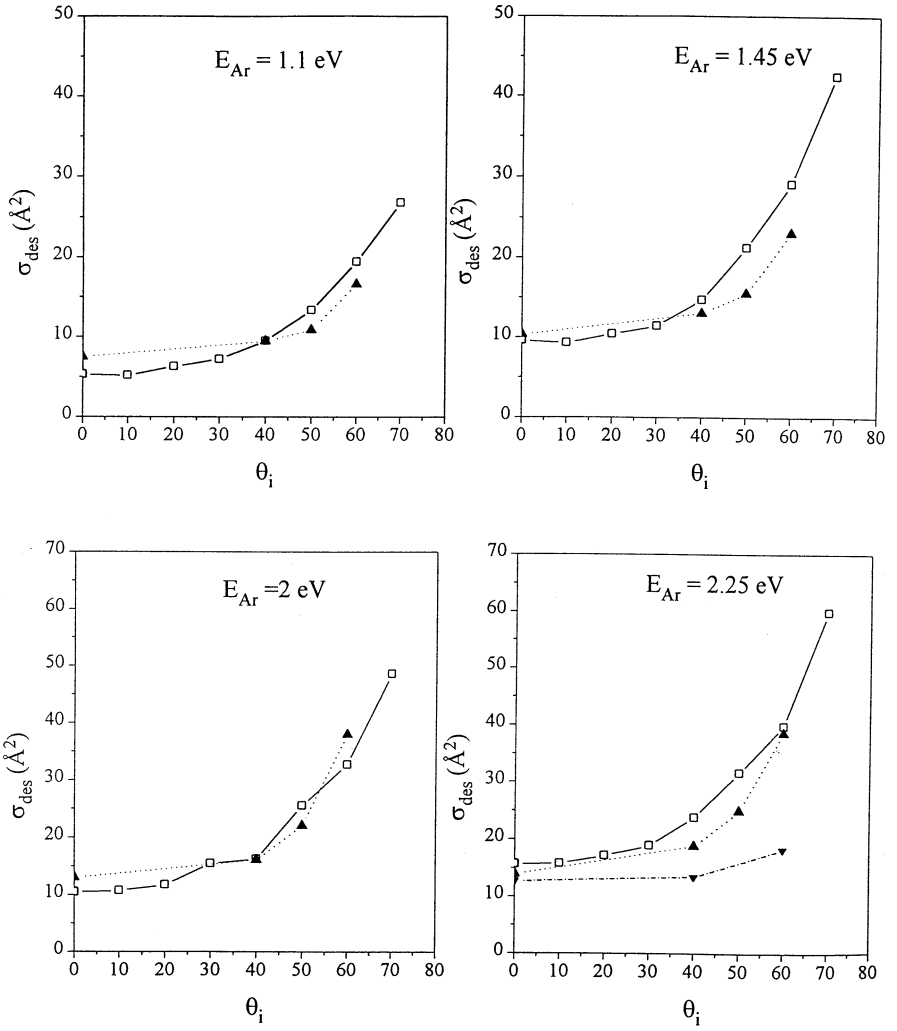

Fig. 2. Experimentally measured (open squares) and calculated (up triangles for normal adsorption geometry and down triangles for parallel adsorption) σ_{des} as a function of incidence angle for the four indicated kinetic energies.

experimental and calculated results for $\sigma_{des}(E_i, \theta_{in} = 0°)$ shows an excellent agreement for incidence energies upto ~ 2.5 eV. Above this E_{in} value the increase of the experimental σ_{des} is faster than the calculated one. To examine the dependence of σ_{des} on the adsorption geometry, simulations were performed at three E_{in} values using parallel adsorption. The calculated σ_{des} for this adsorption geometry are also shown in Fig. 2 as filled down triangles. It is clear that in the E_{in} range examined here the cross section for CID is independent of the adsorption geometry at $\theta_{in} = 0°$.

Another comparison between experimental and calculated results is shown in Fig. 2. Here, the relationship between σ_{des} and the collider incidence polar angle (measured from the surface normal), θ_{in}, θ_i is presented for four E_{in} values. Again, very good agreement between the experimental (open squares) and calculated (filled triangles) data is observed for the case of normal adsorption geometry. For all energy values σ_{des} exhibits a small increase as a function of θ_{in} upto $\theta_{in} = 40°$. For larger incidence angles a rapid increase in the magnitude of the CID cross section

is observed. Calculated cross section values for $E_{in} = 2.25$ eV using parallel adsorption geometry are shown in Fig. 2 for three θ_{in} values. It is clear that for off normal incidence angles the σ_{des} values corresponding to normal adsorption are much larger than those for parallel adsorption.

The good agreement between experimental and calculated results indicates that the semi-empirical PES used in the simulation allows a reliable description of the Ar–N_2–Ru(001) system [9].

The threshold energy (E_{thr}) for desorption is defined as the minimum energy of the collider required to induce desorption. As it follows from this definition, E_{thr} is closely related to the binding energy of the adsorbate. Levis and co-workers [5,6,40–42] proposed a new method to establish the binding energy of an adsorbate based on the experimentally measured E_{thr} for desorption. Employing the hard sphere-hard cube (HSHC) model for CID, the binding energy was calculated by the following equation, as suggested by Kulginov and coworkers [8]:

$$E_{binding} = E_{threshold} \frac{4m_{col}m_{ads}}{(m_{col}+m_{ads})^2}\left[1 - \frac{4m_{ads}m_M}{(m_{ads}+m_M)^2}\right] \times \cos^4\left(\frac{\theta_{in}}{2}\right) \quad (1)$$

where m_{col} and m_{ads} are the collider and adsorbate masses, respectively, m_M is an effective substrate mass, which is equal to a few times of the mass of a surface atom.

The simplified HSHC model provides good agreement with the experimentally measured quantities, E_{thr} ($\theta_{in} = 0°$) and adsorbate–substrate binding energy (E_{bin}) for N_2–Ru(001) system, assuming $m_M = 1.5 \times m_{Ru}$. However, it cannot explain the experimental observation that E_{thr} is independent of the angle of incidence that was found for the N_2–Ru(001) system [9]. Moreover, as follows from Eq. (1), E_{thr} is expected to increase as θ_{in} increases.

An examination of the activation energy for desorption derived from MD simulation, $E_{des} =$ 0.25 eV in our case, as obtained from the definition of E_{thr} for CID, reveals two different experimental values to relate to. Based on TPD data, Menzel and coworkers [10] and Jacobi [11] claimed that the activation energy for desorption is 0.44 eV, while later work by Romm et al. [9] reported $E_{des} = 0.25 \pm 0.05$ eV. Discrepancy in the determination of quantitative values for the activation energy for desorption extracted from TPD data alone are well documented in the literature. Most problematic is the definition of the preexponential factor that often cannot be measured independently. We believe that when CID measurements coupled to MD simulations suggest a value for the activation energy that is about half of the E_{thr} for CID it can be considered dependable. The higher value obtained by Menzel and Jacobi [10,11] is clearly too close to the E_{thr} for CID. Therefore, it seems as if their value for E_{des} is shifted too high by their choice of a rather large preexponential factor. In general, one may use the E_{thr} for CID as an upper limit for the activation energy for desorption, with the later expected to be near half of the E_{thr}. $E_{des} = (0.5 \pm 0.2)\ E_{thr}$.

The total cross section for CID, σ_{des}, was shown by Beckerle et al. [4,5] to increase with θ_{in}. This behavior was related to the faster increase of the geometrical cross section (correlates with $\cos\theta_{in}$) versus the decrease of the normal energy component (correlates with $\cos^2\theta_{in}$), considered to be relevant quantity for CID within the HSHC model. The magnitude of the increase, however, is far too small to explain the results observed in the N_2–Ru (001) system. Moreover, the HSHC model predicts the same results for any adsorbed molecule regardless of the specific details of the molecule–metal interaction potential. This is shown to be incorrect in our case where we compare the two model adsorption configurations of N_2-the normal and the parallel ones. The strong dependence on θ_{in} is observed only in the case of the normal adsorption while the parallel geometry reveals practically no dependence on the angle of incidence, as seen in Fig. 2. The limited ability of the HSHC model to treat polar angle dependence of the CID cross section is further demonstrated in the O_2–Ag(100) system [12,13]. Here, σ_{des} increases by a factor of 40 as θ_{in} increases from normal incidence to 60°. This cannot be explained by any version of the HSHC model.

The variation of the average rotational energy of the nitrogen molecules, $\langle E_{rot} \rangle$, as a function of the incidence angle for five E_{in} values corresponding to normal adsorption and one to parallel adsorption are shown in Fig. 3. In the case of normal adsorption geometry $\langle E_{rot} \rangle$ exhibits a linear decrease for increasing values of θ_{in}. The rate of $\langle E_{rot} \rangle$ decrease varies as a function of E_{in}, namely, larger incidence energy corresponds to a faster decrease of $\langle E_{rot} \rangle$ as a function of incidence angle. A quite different behavior is observed for parallel adsorption geometry. In this case, $\langle E_{rot} \rangle$ exhibits a slow increase when the incidence angle increases. Thus, $\langle E_{rot} \rangle$ at $\theta_{in} = 60°$ is larger by about 25% than the corresponding value at $\theta_{in} = 0°$. These characteristics of the dependence of $\langle E_{rot} \rangle$ on θ_{in} are closely related to the CID mechanism and will be discussed below.

2.2. High coverage

The high coverage simulations were performed using the potential function employed in the low coverage calculations except for the addition of adsorbate–adsorbate interaction term. The magnitude of this additional interaction was estimated from the changes of temperature programmed desorption (TPD) spectra as a function of the initial N_2 coverage on Ru(001). These measurements suggest that, at high coverage, the adsorbed species repel each other [6]. The magnitude of this repulsion was estimated from the shift in the TPD to lower temperatures as the coverage increases. It was found that at monolayer coverage the repulsion among adsorbates results in the reduction of desorption barrier by approximately 1 kcal mol^{-1}. This repulsion was modeled as a sum of pair-wise interactions between Nitrogen atoms belonging to different adsorbates. The N–N pair potential was, thus, described by an exponential function of the form

$$V(R_{N-N}) = A_{rep}\, e^{-\alpha_{rep} R_{N-N}} \quad (2)$$

The magnitude of the parameters A_{rep} and α_{rep} were determined by requiring that the repulsive energy corresponding to a full mono-layer of Nitrogen molecules will reproduce the experimentally observed reduction in adsorbate–substrate binding. The values of these parameters as used in the simulations were: $A_{rep} = 1$ eV and $\alpha_{rep} = 0.715$ $Bohr^{-1}$. The adsorbate–adsorbate interaction, using Eq. (2) indeed results in a decrease of 1 kcal

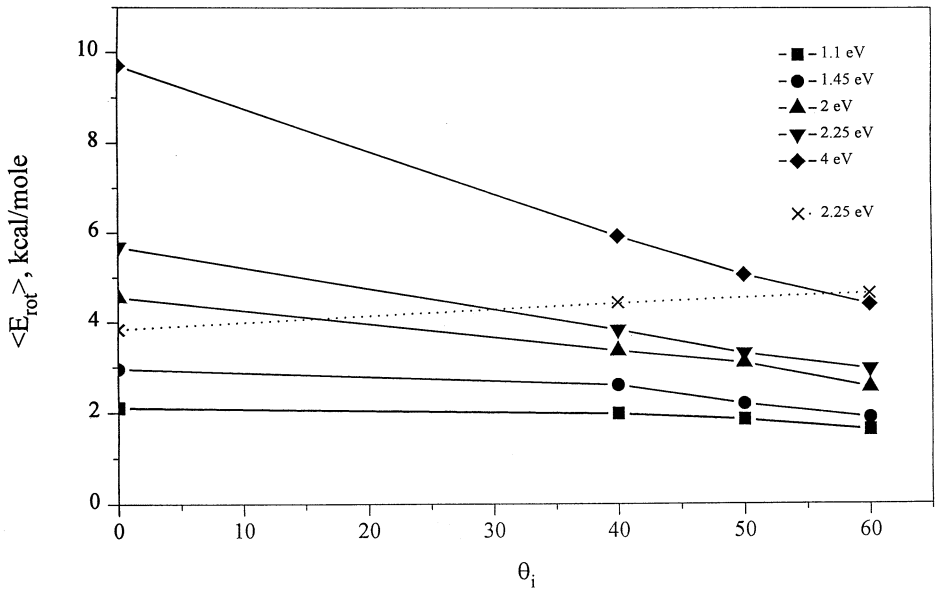

Fig. 3. Average rotational energy $\langle E_{rot} \rangle$ as a function of θ_{in} for different E_{in}. The results obtained for parallel adsorption case are shown for comparison (crosses).

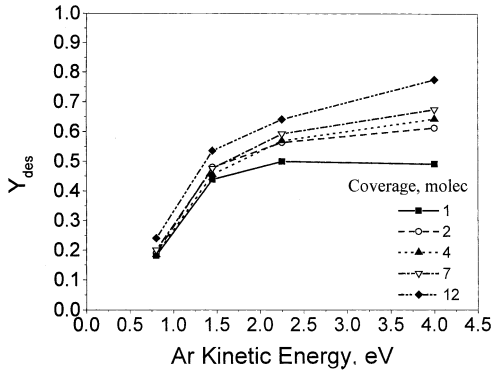

Fig. 4. Variation of desorption yield as a function of incidence projectile energy for five different coverages (designated by the number of adsorbates, N_{ad}). $N_{ad} = 12$ correspond to mono-layer coverage.

mol^{-1} in the adsorbate–surface binding energy at the completion of a mono-layer (12 adsorbed molecules on the slab in the present simulations).

The cross sections for CID at low coverage, σ_{des}, were calculated using the opacity function obtained from the MD simulations. The calculation of σ_{des} is meaningful only if there exists an impact parameter value, b_{max}, above which the opacity function becomes zero. This requirement was fulfilled in the study of the low coverage limit where a single adsorbate was considered. The value of b_{max} was found to depend on the incidence angle of the projectile but in all cases was larger than 3.5 Å. This value is of the order of the nearest neighbor adsorbate–adsorbate distance at high coverage. As a result, the opacity function is not expected to decrease to zero and cannot be used to calculate the cross section for the CID process at high coverage values. Hence, in the present study rates of CID will be related to the desorption yield, Y_{des}, defined by the ratio between the number of desorbates, N_{des}, obtained in the calculation of all trajectories N_{traj} (i.e. number of projectiles considered).

The variation of Y_{des} as a function of projectile translational energy at normal incidence is shown in Fig. 4 for five different coverage values. For all coverage values desorption yield exhibit a rapid initial increase as a function of E_{in}, upto approximately $E_{in} = 1.75$ eV. At higher energies, Y_{des} increases less rapidly and tends to converge to a saturation value. The value of Y_{des} at saturation increases as a function of initial coverage. The increased desorption yields as a function of coverage, for a given E_{in} value, is due to three reasons.

1. The repulsive interaction among the adsorbates results in a decreased adsorbate–substrate binding. Thus, a given amount of energy transferred from the collider to an adsorbate is expected to result in a larger desorption probability when the coverage is increased. It should be noted that based on the experimental findings the adsorbate to substrate binding decreases by about 1 kcal mol^{-1} when coverage is increased to full mono-layer. As a result we expect that the E_{thr} for CID at mono-layer coverage would be somewhat lower than that at the low coverage limit. Indeed, the results presented in Fig. 1 show that E_{thresh} for mono-layer of adsorbates is smaller by about 10% as compared with the value obtained for low coverage (0.5 eV, see [9–11,34]).
2. The effective corrugation along the surface felt by an adsorbate increases as a function of coverage. Increase in the potential corrugation results in a more efficient transfer of adsorbate energy from its translational modes along the surface to the one normal to the surface, hence, desorption probability increases.
3. At high E_{in} values, the probability to obtain multiple desorption events as a result of a single collision increases with the projectile kinetic energy, incidence (polar) angle and the initial surface coverage.

These features are closely related to the desorption mechanism and will be further discussed below.

Next we examine the response of Y_{des} to a change in the incidence polar angle, θ_{in}, at which the collider approaches the surface. The results corresponding to $E_{in} = 4$ eV are shown in Fig. 5 for the same five coverages as in Fig. 4. It is clear that at the low coverage limit only a very weak dependence of the desorption yield on θ_{in} is observed. When off normal incidence angles are used Y_{des} increases by a few percent only. It should be noted that the cross section for CID was found to increase, in this θ_{in} range, by a

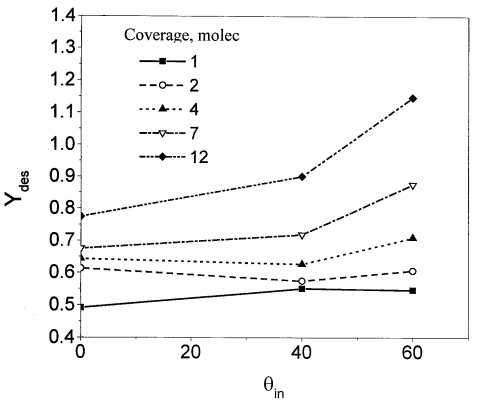

Fig. 5. CID yield as a function of incidence angle at five different surface coverages.

factor of approximately four [9–11,32,33]. At the low coverage range, variation of θ_{in} result mainly in the increase of successful CID events at large impact parameters. But at the same time a corresponding decrease is found in the yield of CID events at the small impact parameter regime. These two trends almost exactly cancel each other, thus, leading to the observed insensitivity to θ_{in}. At the highest coverage, on the otherhand, Y_{des} increases by 50% when θ_{in} changes from 0 to 60°. Moreover, at mono-layer coverage the desorption yield is larger than unity for $\theta_{in} = 60°$. In this case, a significant fraction of the trajectories end up ejecting more than a single adsorbate. The results shown in Fig. 5 clearly demonstrate the non-uniform dependence of Y_{des} on θ_{in} for different initial coverage values. For example, Y_{des} for mono-layer coverage increases by 60% as compared with the corresponding value at the low coverage for normal incidence, while for $\theta_{in} = 60°$ the ratio between the desorption yields at mono-layer and low coverage increases by more than a factor of two.

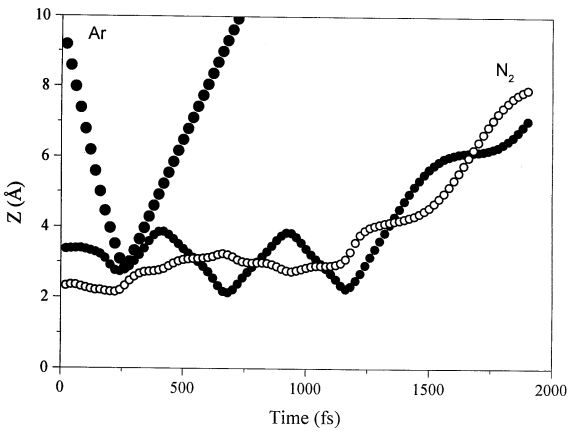

Fig. 6. A typical CID trajectory. The two ends of the nitrogen molecule are shown as open and filled circles.

The sequence of collision events of the projectile at off normal angle of incidence is quite different. In this case the collider normal energy component is much smaller, hence, its turning point correspond to larger Ar-substrate distances. Similar to the case discussed above, the interaction between the rare-gas atom and the nearest target adsorbate results in the deflection of the projectile from its original trajectory. If this deflection results in a sign change in the projectile normal velocity component it will proceed to the gas-phase without additional collisions with other adsorbates. Such trajectories can be viewed as glancing collision of the collider from the adsorbate layer. The amount of energy transferred between the projectile and the target adsorbate is determined by the magnitude of the impact parameter, b. Kinematically, for near zero b the projectile may lose about 90% of its energy to the target N_2, however, for large impact parameters the amount of energy transfer becomes much smaller. While the glancing collisions constitute a small fraction of the trajectories studied, in most cases the projectile interacts with a number of adsorbates before it is scattered back to the gas-phase. For such trajectories one expects the collider to lose a large fraction of its initial energy to the adsorbates layer. Again, the interaction between the adsorbates should result in some degree of redistribution of the energy among the target adsorbates and their nearest neighbors.

2.3. CID mechanism

In order to gain insight into the details of the CID mechanism a large number of individual trajectories with different impact parameter values were carefully examined for the energy range $E_{in} = 0.8–5.5$ eV and both normal and off normal

angle of incidence. A typical example for $E_{in} =$ 4eV is shown in Fig. 6. As the projectile approaches the adsorbed nitrogen molecule, the repulsion between the collider and upper N atom rises and causes the molecule to tilt and bend towards the surface plane approaching a parallel geometry. The adsorbate acquires the largest torque when the collision geometry is not line-of-centers, but with the impact parameter in the range 1–1.5 Å. Here, the collision between projectile and adsorbate results in a large amount of energy transferred into the frustrated rotational mode of the adsorbed molecule as well as into translation parallel to the surface (note the large polar angle at which the desorbate leaves the surface, θ_{out}). Part of the energy in these two modes is transferred into kinetic energy in the direction normal to the substrate that in turn leads to desorption. The energy transfer into motion along the surface normal is possible due to the coupling of this mode with the frustrated rotation and parallel motion modes by the corrugation of N_2–Ru PES. Detailed dynamic picture of the kind discussed above is of course impossible within the HSHC model, where parallel momentum is assumed constant.

For off normal incidence the motion of molecule parallel to the surface prior to its desorption becomes more probable. The parallel momentum transfer from the incoming Ar atom into translational and rotational modes of the adsorbed N_2 molecule leads to the tumbling of the adsorbate along the surface [32]. This motion is again coupled to the motion normal to the surface by virtue of the PES corrugation.

Thus, the dominant mechanism of the CID is direct impulsive bimolecular collision, in which collider energy is transferred into the frustrated rotation of the adsorbate, its kinetic energy along the surface plane, and into the surface. Although the amount of energy transferred into each of these channels is dictated by the collision geometry, the energy acquired by the adsorbate upon collision is effectively channeled by the corrugated molecule-surface PES into the motion normal to the surface. At normal incidence as a result of significant excitation of the frustrated rotation this degree of freedom is kept by the molecule all the ways to the gas phase following desorption. At off normal incidence the frustrated rotation is less important in the CID sequence, and desorbate leaves the surface rotationally colder. Meanwhile, at off normal incidence the kinetic energy of the collider more effectively channels into the kinetic energy of the desorbate, and the latter leaves the surface translationally more excited relative to the normal incidence case.

At high coverages, the effect of neighboring molecular interactions on the desorbate kinetic energy, rotational energy and angular distributions were determined. Vibrational excitations following the CID event were not observed in the MD simulations, however, efficient rotational energy excitation is predicted which depends on both incident energy and angle of incidence. Polar and azimuthal angular distributions were found to be strongly dependent on the incidence angle and energy of the colliders. These distributions are very similar to those obtained at the low coverage limit, indicating the dominance of the local potential over interactions with neighboring adsorbates. In general, neighboring molecules act to focus the desorbing ones closer to the normal to the surface and broaden the energy distributions.

3. Collision induced migration (CIM)

The effect of energetic colliders on surface processes such as desorption (CID) [1,3,6,8,9,31,43] and reaction (CIR) [4,19] have been demonstrated. These processes were considered as possible new routes for surface reactivity in industrial catalysis, where energetic gas phase molecules in the tail of the Boltzmann distribution can affect the heterogeneous catalytic processes [1,3,31].

With this background of collision induced surface processes that have already been investigated, it is rather surprising to realize that the far more probable CIM has never been considered neither theoretically nor experimentally. The results discussed below are based on MD simulations. The data correspond to CIM of adsorbed nitrogen molecules on Ru(001) at 90 K following collisions with gas phase argon atoms. The complimentary study of CID of N_2 from Ru(001) has been discussed above.

In the following, we define as target adsorbate (TM) the molecule directly hit by the collider. In all the simulations the TM was chosen as the adsorbate positioned at the shortest distance from the slab center. In Fig 9 a–c the average migration distance (AMD) of the target molecule (TM) is shown for increasing impact parameters at $E_{in} = 1.45$ eV, $\theta_{in} = 0$, 40, 60°, for the indicated initial coverage values. We define the AMD as the distance between the position of the TM at $t = 0$ and its position after 10 ps, averaged over impact parameters within a given range. The AMD is defined here for all the trajectories that were found to be non-desorbing during 10 ps. The results clearly show that at normal incidence maximum displacement of the TM is reached at non-zero impact parameter, $b_{imp} \approx 1°$. At this collision geometry the energy transferred from the projectile to the adsorbate is channeled most effectively into lateral migration of the adsorbate. At other angles of incidence (40° and 60°), trajectories having $b_{imp} \approx 0$ Å are the most effective to induce long migration distances. A strong dependence of AMD on θ_{in} is observed. The migration distances shown in Fig. 7 reflect the remarkable efficiency of the CIM process in this system.

As coverage increases the AMD significantly shortens while the CIM process attenuates. This is a direct consequence of the multiple inter–adsorbates collisions between the TM and its neighbor adsorbates, which block the original direction of motion of the TM on the surface. For all these angles of incidence, the AMD decreases by nearly an order of magnitude when the coverage increases from 1 ($\Theta = 0.018$) to 12 ($\Theta = 0.21$) molecules on the slab.

To estimate how the CIM process can be followed experimentally, one has to integrate the AMD values (IAMD) shown in Fig. 7 over the entire impact parameter range. The values of IAMD obtained this way were then calculated for different coverage values as a function of Ar kinetic energy. The results are shown in Fig. 8 for two angles of incidence, $\theta_{in} = 0$ and 60°.

These results clearly show that the integrated AMD is about a factor of 5 shorter than the corresponding AMD. Moreover, the energy dependence is quite modest as compared with that

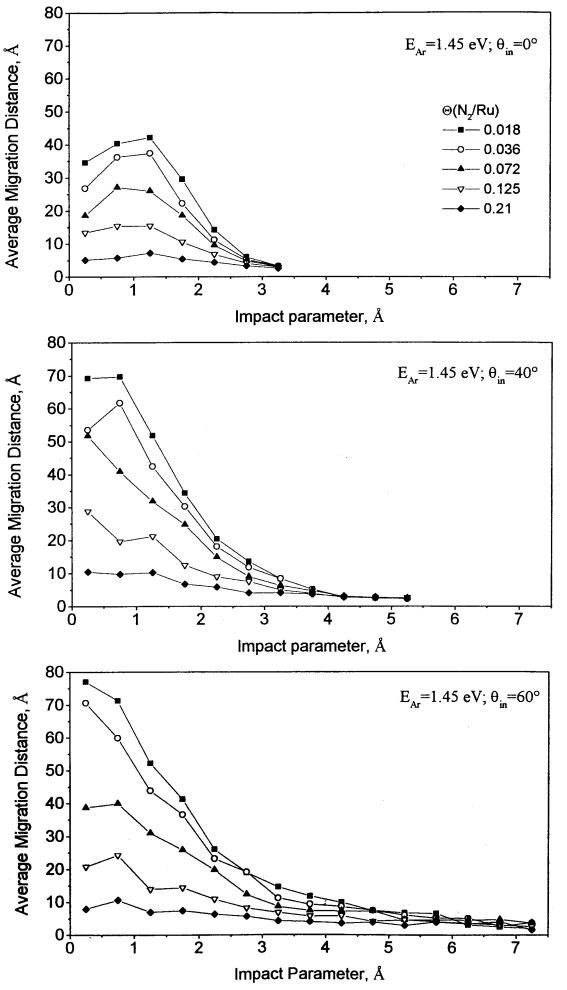

Fig. 7. AMD vs. impact parameter.

obtained for AMD. The reason for this behavior is that there are many more Ar trajectories at large impact parameters which result in small AMD than those with small impact parameters and large AMD. As the collision energy increases, AMD values at small impact parameters increase, but at the same time the number of trajectories at large impact parameters also increase. The net result is a compensation effect, process which diminish the overall efficiency and energy dependence of the CIM.

It was found that single adsorbed molecule can migrate over 150 Å following collisions at high energies and large angles of incidence. As cover-

age increases, inter-adsorbate collisions efficiently quench the migration distance. At high energies, the competing CID becomes dominant, leaving behind only low energy adsorbates which migrate to relatively short distances. This results in an optimum collision energy for the most efficient CIM process near 2.0 eV. It was observed that the target molecule migrates for long distances due to the fact that its center of mass is found to reside more than 0.5 Å above its equilibrium adsorption position for 2–5 ps, during which it has a very small barrier for diffusion [33]. An interesting open question that arises from this study and needs to be addressed in the future is the conceptual similarity and difference between CIM and thermal diffusion.

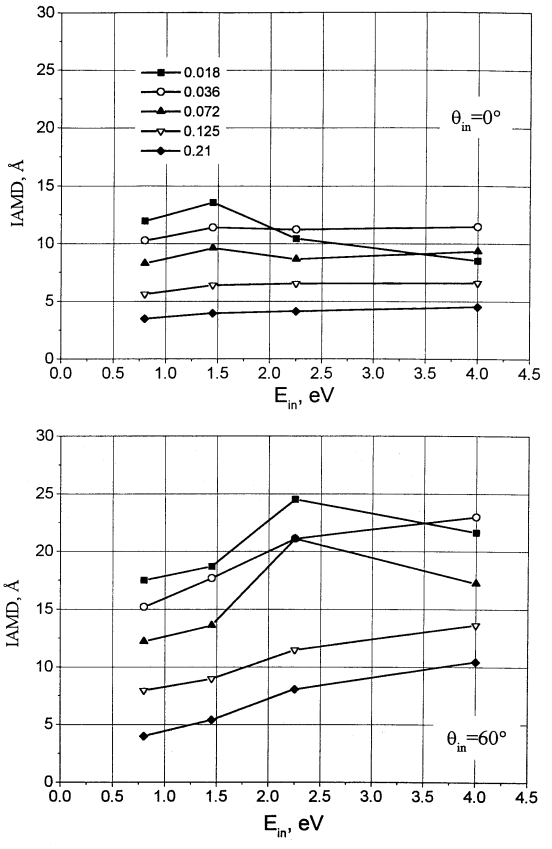

Fig. 8. Variation of the integrated AMD as a function of the collider's incidence kinetic energy for five different coverages (noted on the upper panel) and two angles of incidence: $\theta_{in} = 0°$ (upper panel) and $\theta_{in} = 60°$ (lower panel).

4. Conclusions

A number of different CIP were described and analyzed. The first process considered was the CID of N_2 from the Ru(001) surface. The experimental data suggested that, in the limit of low coverage, the CID cross section increases as a function of projectile incidence energy and seems to converge at high E_{in} to a saturation value. In addition, the CID process was found to exhibit a E_{thr} below which no desorption is detected. The magnitude of the E_{thr} was found to be about twice the binding energy of nitrogen to Ru(001). The experimental results also indicated that the E_{thr} is independent of the incidence angle of collider suggesting that normal energy scaling is not applicable in this case. At a given E_{in}, the CID cross section was found to increase as a function of θ_{in} yielding values larger by a factor upto four at incidence angle of 60° as compared with normal incidence.

The detailed understanding of the CID results was obtained using MD simulations. Very good qualitative (and semi quantitative) agreement was obtained between the experimental and theoretical data, suggesting that the PES used to describe the system is reliable. The MD calculations indicated that the desorption mechanism involves energy transfer among desorbate modes due to potential corrugation and coupling between translational and frustrated rotational motions. Similar desorption mechanism was found to operate in the case of high coverage. In the case of high coverage the desorption yields increased and for grazing collisions, $\theta_{in} = 60°$, we obtained desorption yields larger than unity. These results suggest that some of the projectiles lead to desorption of more than a single adsorbate.

The MD simulations also exhibited the occurrence of CIM process. It was found that at low coverage the CIM process could result in extremely long migration distances of the target adsorbates. This migration distance decreases markedly when surface coverage is increased to a mono-layer. It is argued that the CIM process can play an important role in various surface reactions where the mixing between two (or more) reactants is required.

Acknowledgements

This work has been partially supported by a grant from the Israel Science Foundation and by the German Israel Foundation. The Farkas Center for Light Induced Processes is supported by the Bundesministerium für Forschung und Technologie and the Minerva Gesellschaft für die Forschung mbH.

References

[1] Y. Zeiri, J.J. Low, W.A. Goddard, J. Chem. Phys. 84 (1986) 2408.
[2] W.J. Hays, W.E. Rogers, E.L. Knuth, J. Chem. Phys. 56 (1972) 1652.
[3] J.D. Beckerle, A.D. Johnson, S.T. Ceyer, Phys. Rev. Lett. 62 (1989) 685.
[4] J.D. Beckerle, A.D. Johnson, S.T. Ceyer, J. Chem. Phys. 93 (1990) 4047.
[5] G. Szulczewski, R.T. Levis, J. Chem. Phys. 98 (1993) 5974.
[6] G. Szulczewski, R.T. Levis, J. Chem. Phys. 103 (1995) 10238.
[7] L. Romm, T. Livneh, M. Asscher, J. Chem. Soc. Faraday Trans. 91 (1995) 3655.
[8] D. Kulginov, M. Persson, C.T. Rettner, J. Chem. Phys. 106 (1997) 3370.
[9] L. Romm, Y. Zeiri, M. Asscher, J. Chem. Phys. 108 (1998) 8605.
[10] P. Feulner, D. Menzel, Phys. Rev. B 25 (1982) 4295.
[11] K. Jacobi, Phys. Status Solidi, A 177 (2000) 37.
[12] L. Vattuone, P. Gambardella, F. Cemic, U. Valbusa, M. Rocca, Chem. Phys. Lett. 278 (1997) 245.
[13] L. Vattuone, P. Gambardella, U. Burghaus, F. Cernic, A. Cupolillo, U. Valbusa, M. Rocca, J. Chem. Phys. 109 (1998) 2490.
[14] J.D. Beckerle, Q.Y. Yang, A.D. Johnson, S.T. Ceyer, J. Chem. Phys. 86 (1987) 7236.
[15] J.D. Beckerle, A.D. Johnson, Q.Y. Yang, S.T. Ceyer, J. Chem. Phys. 91 (1989) 5756.
[16] E. Por, M. Asscher, J. Chem. Phys. 90 (1989) 3405.
[17] C. Akerlund, I. Zoric, B. Kasemo, J. Chem. Phys. 109 (1998) 737.
[18] P. Lohokare, E.L. Crane, L.H. Dubois, R.G. Nuzzo, J. Chem Phys. 108 (1998) 8640.
[19] C. Akerlund, I. Zoric, B. Kasemo, J. Chem. Phys. 104 (1996) 7359.
[20] K.L. Haug, T. Burgi, T.R. Trautman, S.T. Ceyer, J. Am. Chem. Soc. 120 (1998) 8885.
[21] Q.Y. Yang, K.J. Maynard, A.D. Johnson, S.T. Ceyer, J. Chem. Phys. 102 (1995) 7734.
[22] A.D. Johnson, S.P. Daley, A.L. Utz ans, S.T. Ceyer, Science 257 (1992) 223.
[23] I. Harrison, J.C. Polanyi, P.A. Young, J. Chem. Phys. 89 (1988) 1498.
[24] E.B.D. Bourdon, C.C. Cho, P. Das, J.C. Polanyi, C.D. Stanners, G.Q. Xu, J. Chem. Phys. 95 (1991) 1361.
[25] Q.S. Xin, X.Y. Zhu, Surf. Sci. 347 (1996) 346.
[26] X.Y. Zhu, Surf. Sci. 390 (1997) 224.
[27] I. Harrison, V.A. Ukraintsev, A.N. Artsyukhovich, SPIE 285 (1994) 2125.
[28] A.N. Artsyukhovich, I. Harrison, Surf. Sci. 350 (1996) L199.
[29] Y. Zeiri, J. Chem. Phys. 112 (2000) 3408.
[30] J.C. Polanyi, Y. Zeiri, in: H.ai-L.ung Dai, W. Ho (Eds.), Laser Spectroscopy and Photo-Chemistry on Metal Surfaces, World Scientific, Singapore, 1995 and references therein.
[31] Y. Zeiri, Surf. Sci. 231 (1990) 404.
[32] L. Romm, M. Asscher, Y. Zeiri, J. Chem. Phys. 110 (1999) 3153.
[33] L. Romm, M. Asscher, Y. Zeiri, J. Chem. Phys. 110 (1999) 11023.
[34] J.T. Kindt, J.C. Tully, J. Chem. Phys. 111 (1999) 11060.
[35] Y. Zeiri, R.R. Lucchese, J. Chem. Phys. 94 (1991) 4055.
[36] Y. Zeiri, R.R. Lucchese, Surf. Sci. 264 (1992) 197.
[37] S.T. Ceyer, Science 249 (1990) 133.
[38] G.A. Somorjai, Introduction to Surface Chemistry and Catalysis, Wiley, New York, 1994.
[39] Y. Zeiri, J. Chem. Phys., 113 (2000) 3868.
[40] D. Velic, R.J. Levis, J. Chem. Phys. 104 (23) (1996) 9629.
[41] D. Velic, R.J. Levis, Chem. Phys. Lett. 269 (1996) 59.
[42] D. Velic, R.J. Levis, Surf. Sci. 396 (1998) 327.
[43] C. Akerlund, I. Zoric, B. Kasemo, A. Cupolillo, F. Buatier de Mongeot, M. Rocca, Chem. Phys. Lett. 270 (1997) 157.